IEEE Access
Multidisciplinary | Rapid Review | Open Access Journal

Received November 20, 2019, accepted December 23, 2019, date of publication January 1, 2020, date of current version January 17, 2020.

Digital Object Identifier 10.1109/ACCESS.2019.2963458

Regional Assessment of Climate Potential Productivity of Terrestrial Ecosystems and Its Responses to Climate Change Over China From 1980-2018

DAN CAO[1,2], JIAHUA ZHANG[1,2], HAO YAN[3], LAN XUN[1,2], SHANSHAN YANG[1,2], YUN BAI[4], SHA ZHANG[4], FENGMEI YAO[2], AND WENBIN ZHOU[5]

[1]Key Laboratory of Digital Earth Science, Aerospace Information Research Institute, Chinese Academy of Sciences, Beijing 100094, China
[2]College of Earth and Planetary Sciences, University of Chinese Academy of Sciences, Beijing 100049, China
[3]National Meteorological Center, China Meteorological Administration, Beijing 100081, China
[4]Remote Sensing Information and Digital Earth Center, College of Computer Science and Technology, Qingdao University, Qingdao 266071, China
[5]Institute of Crop Sciences, Chinese Academy of Agricultural Sciences, Beijing 100081, China

Corresponding authors: Jiahua Zhang (zhangjh@radi.ac.cn) and Fengmei Yao (yaofm@ucas.ac.cn)

This work was supported in part by the National Key Research and Development Program of China under Grant 2016YFD0300110 and Grant 2016YFD0300101, in part by the CAS Strategic Priority Research Program under Grant XDA19030402, in part by the Natural Science Foundation of China under Grant 31671585 and Grant 41871253, in part by the Key Basic Research Project of Shandong Natural Science Foundation of China under Grant ZR2017ZB0422, in part by the Shandong Key Research and Development Project under Grant 2018GNC110025, in part by the "Taishan Scholar" Project of Shandong Province under Grant TSXZ201712, and in part by the Science Foundation of Hebei Normal University under Grant 130539.

ABSTRACT Evaluating the potential productivity of the terrestrial ecosystem is extremely important to ascertain the threshold of vegetation productivity, to maximize the utilization of regional climate resources, carbon sequestration and to mitigate climate warming caused by rising CO_2 concentrations. However, most previous studies neglected the optimum state of natural vegetation without human intervention and regional change trend of vegetation under future climate change. In this study, variations in spatio-temporal distributions of climate potential productivity (CPP) over China from 1980 to 2018 are analyzed with the synthetic estimating model. A comprehensive regionalization method (Principal components analysis, PCA) based on standardized precipitation evapotranspiration index (SPEI), and statistical analysis methods are adopted to assess CPP and its response to the climate change in different regions of China. The results demonstrate that the global temperature rising and precipitation decreasing have obvious effects on the productivity of terrestrial ecosystem and its spatio-temporal distribution in different sub-regions and ecosystems. Among them, precipitation is the dominant factor, and temperature significantly affects some regions such as Tibetan Plateau (TP) and Northeast China (NE) with high-altitude or high-latitude. The optimum temperature for the CPP in Xinjiang (XJ) region and Northwest China (NW) is 7.5°C and 8°C, respectively. With regards to the ecosystems, the CPP of grassland shows complex trends in XJ, Southwest China (SW), NE, and TP; especially in XJ (NE), the CPP shows a decreasing (an increasing) trend when the temperature is more than 7.5°C (0°C). Linear correlations occur between farmland CPP and temperature in each sub-region except for XJ. The same situation also exists at forest CPP, especially in TP, NE and NC regions. However, under the temperature increasing and precipitation decreasing, there are slight adverse impacts on the CPP of vegetation at the national scale, indicating that drier and warmer climate are detrimental for vegetation growth.

INDEX TERMS Climate potential productivity (CPP), synthetic model, SPEI, spatio-temporal variation, climate change.

I. INTRODUCTION

Climate change leads to variations in the global distribution of surface temperature and precipitation, which has a profound influence on regional resource allocation, carbon and water

The associate editor coordinating the review of this manuscript and approving it for publication was Jenny Mahoney.

cycles of terrestrial ecosystems [1]–[3]. Many studies point out that climate is the most critical factor that determines the distribution pattern and structural characteristics of terrestrial vegetation types. And some of them show that a shrinking natural resource is suffering from climate change [4]–[7]. Optimum utilization of regional climate resources is an urgent need for ecosystem protection and management under the background of climate change. Climate potential productivity (CPP) represents the vegetation can make full use of the climate resources, such as light, heat and water when other factors are in the optimum state, which can obtain the maximum biological or economic yield produced by photosynthesis per unit area and per unit time [5], [8]–[10]. Therefore, understanding the CPP of vegetation can not only reveal the relationship between productivity and climate factors but also predict the future development of vegetation production capacity according to the trend of global climate [11]–[14].

Generally, CPP defined as the maximum regional net primary productivity (NPP) is difficult to estimate, which is just affected by climate factors. Many endeavors have been devoted to using meteorological factors as driving parameters for simulating CPP, such as Miami model [10], Thornthwatite Memorial model [10] and Chikugo model [15]. Studies have shown that these statistic models have their respective applicability in different regions and that they are all suitable for the eco-environment with abundant water and flourishing vegetation [16]. For example, Li *et al.* [17] and Li [18] used Miami model and Thornthwatite Memorial model simulated CPP of Yunnan Province and Central Asia, respectively, which showed that the warm and wet would be beneficial for production in the future. Guo *et al.* [19] calculated CPP of spring maize and found that adjusting cropping systems could dominantly contribute to utilization efficiency increases of agricultural climatic resources in Northeast China in the future. However, there are many uncertainties of CPP estimation in the arid and semi-arid regions, where CPP tends to be overvalued [20]. Besides, the increasing studies on estimation of NPP are based on remote sensing data and process-based models, such as the BIOME-BGC [21] and light use efficiency (LUE) models, i.e., CASA model [22], [23]. However, studies show that these models are more suitable for estimating actual regional NPP. The process-driven models always require complicated parameters, such as soil property and physiological parameters. Hence, the climate-based synthetic model runs mainly by annual average temperature and precipitation data, which conquers the data deficiency and parameterization problems, especially in the data scare regions.

There are various climatic zones in China: cold temperate, middle temperate, temperate, subtropical, and tropical zones extending from north to south, with numerous vegetation types [24]. Interactions between vegetation and climate changes vary in different climate zones and vegetation types. Regional CPP assessment can adequately reflect the differences in trends and spatiotemporal characteristics of regional vegetation responses to climate change. CPP of terrestrial ecosystems may be influenced by droughts directly related to temperature increase and precipitation decrease [25], [26]. Therefore, studying the trend of vegetation change in the area according to drought conditions can well reflect the response of vegetation to water and heat condition. The SPEI (standardized precipitation evapotranspiration index) is developed to monitor droughts, which considers both the sensibility of droughts to temperature and the effect of precipitation [27], [28]. Consequently, regionalization based on SPEI can effectively reflect the temperature and precipitation effects in different regions and ecosystems. Generally, the SPEI values at different timescales (3-month, 6-month, 12-month and 24-month scale) have different sensibilities to the dry/wet condition. For example, 3-month time scale can reflect the meteorological drought, 6-month time scale can reflect the agricultural ecological drought, and 12-month time scale can reflect the long-term hydrological drought [29], [30]. The 12-month SPEI (SPEI-12) can maintain the characteristics of inter-annual variation, and avoid the seasonal cycle [31], while the shorter time scales such as 3-month or 6-month scale are too vulnerable and the longer time scales (24-month) may easily miss some serious drought events [32]. Here, we divide the study area into several sub-regions based on drought (SPEI-12) and then assess the CPP and its responses to climate change at a regional scale.

Many previous studies have evaluated the responses of the terrestrial ecosystem to climate change in existing regions [33], [34], but have not assessed regional differences in terms of the effects of temperature and precipitation on drought. In addition, the threshold of vegetation productivity and the potential influences of the natural vegetation on climate change have not been explored. To address this challenge, this paper explores the spatio-temporal variation of CPP in different sub-regions of China from 1980 to 2018 using SPEI based on PCA (Principal components analysis) methods. Furthermore, the responses of the terrestrial ecosystem potential productivity to temperature and precipitation are analyzed using trend analysis and correlation coefficients analysis methods.

II. MATERIALS AND METHODS

A. STUDY AREA

China, the third-largest county in the world, locates in East Asia and on the western shore of the Pacific Ocean (Fig. 1a). Temperate monsoon climate, subtropical monsoon climate, tropical monsoon climate, tropical rain climate, temperate continental climate, and plateau mountain climate dominates different regions in China, and the climate diversity results in various vegetation types [24]. Meanwhile, China is divided into the southeastern and the northwestern parts. The southeastern part belongs to the monsoon climate zone and its vegetation reflects the zonal regularity. The tropical monsoon rain, evergreen broad-leaved, deciduous broad-leaved in the warm temperate zone, broad-leaved, mixed coniferous and coniferous are found successively from south to north.

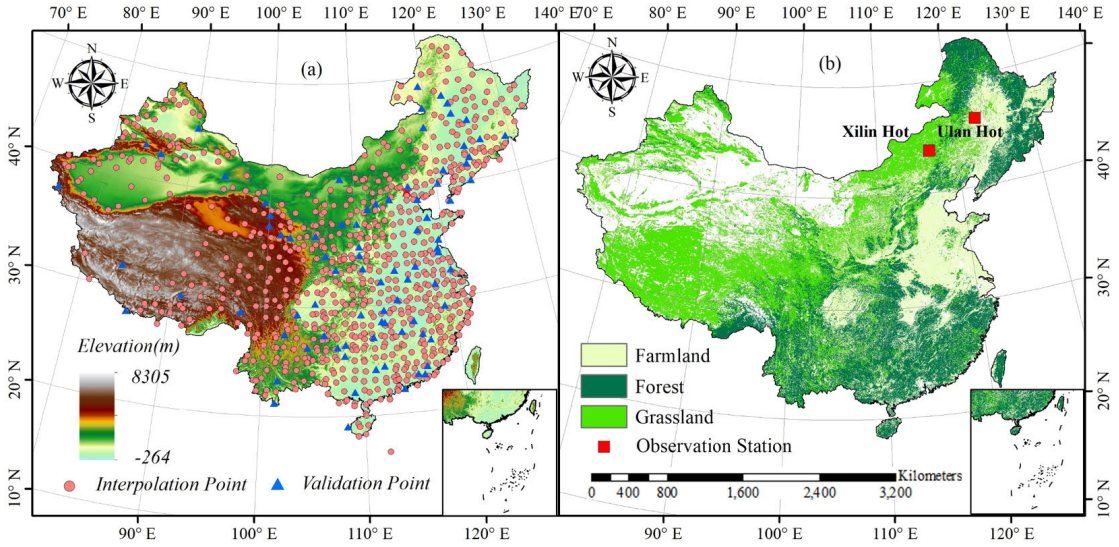

FIGURE 1. (a) DEM of China and the meteorological stations, the pink circles (90% of the total number of stations) are used to interpolation and the blue triangles (10% of the total number of stations) are used to verify the accuracy of interpolation. (b)The major three ecosystems used in this study.

There is a weak impact of northwestern monsoon on the distribution of grassland and desert. The topography in China is high in the west and low in the east, complex and diverse. Different topography has a remarkable influence on the growth and richness of vegetation.

B. DATA PROCESSING

The meteorological data, including daily temperature and daily precipitation from 1980 to 2018 are used in the study. All data are collected from the National Meteorological Information Center (http://data.cma.cn/), and 664 meteorological stations are selected from the whole country in the current study. The meteorological data are used to drive the CPP estimating model including yearly mean temperature and yearly precipitation datasets. Additionally, monthly mean temperature, precipitation datasets and the latitude of every station are employed to calculate the SPEI. These data are interpolated to produce regular yearly and monthly raster data with 1km spatial resolution.

Land use maps of China (2015) are derived from the Resource and Environment Data Cloud Platform (http://www.resdc.cn/). The datasets are classified into six land cover classes based on Landsat 8 remote sensing images, including grassland, forest, farmland, water area, residential land, and unused land. The derived data are projected into the same projection (Albers equal area projection). The grassland, forest, and farmland are the top three major vegetation types, which are extracted to analyze the response of different terrestrial vegetation ecosystems to climate change (Fig. 1b).

DEM data with 1km resolution are derived from the Resource and Environment Data Cloud Platform (http://www.resdc.cn/) (Fig. 1a), which is mainly used for meteorological data interpolation as influencing factors of temperature and precipitation. In-situ data are primarily collected by the Distributed Active Archive Center For Biogeochemical Dynamics (ORNL DAAC) Net Primary Production database (http://daac.ornl.gov/NPP/npp_home), which is especially helpful for modeling and testing hypothesis [35].

C. METHODS

1) ESTIMATION OF CPP

According to the physiological and ecological characteristics of plants and the regional evapotranspiration model based on the energy balance equation and the water balance equation, Zhou [20] and Zhang [36] established a synthetic model to estimate NPP. The maximum regional productivity of the calculated NPP result is identified as potential productivity [5]. The calculation formula is established mainly based on the measured biomass data, which is from 125 stations connected with natural mature and 23 stations related to natural vegetation NPP in China such as grassland, forest and desert. The calculation formulae are as follows [20], [36]:

$$NPP = 100 \times RDI \frac{rR_n(r^2 + R_n^2 + rR_n)}{(R_n + r)(R_n^2 + r^2)} \times \exp(-\sqrt{9.87 + 6.25RDI}) \quad (1)$$

$$R_n = RDI \times r \times L \quad (2)$$

$$RDI = (0.629 + 0.237 \times PER - 0.00313 \times PER^2)^2 \quad (3)$$

$$PER = \frac{PET}{r} = \frac{BT \times 58.93}{r} \quad (4)$$

$$BT = \frac{\sum t_d}{365} \quad (5)$$

$$L = 597 - 0.6T_m \quad (6)$$

where r is annual precipitation, R_n is annual net radiation, RDI is radiant dryness, L is potential heat of evaporation, PET is latent evapotranspiration, PER is probably evapotranspiration rate. Biological temperature (BT) is the average temperature in the plant vegetative growth, generally between 0 and 30°C. Mean daily temperature (t_d) and mean monthly temperature (T_m) take 0°C when it is lower than 0°C and 30°C when the temperature is above 30°C. The unit of NPP calculated by the above formulas is g DW $\cdot$ m^{-2} $\cdot$ a^{-1}. Thus, the final result needs to multiply a conversion factor (0.475) [37] in China from dry matter (DW) to carbon content (g C $\cdot$ m^{-2} $\cdot$ a^{-1}).

2) CALCULATION OF SPEI

In this study, the SPEI at 12-month timescales (SPEI-12) as an indicator of regional division is selected to depict the different wet and dry conditions in different regions from 1980 to 2018 over China. The calculation formulae are as follows:

$$D_j = P_j - PET_j \tag{7}$$

$$\begin{cases} X_{t,j}^{12} = \sum_{l=1+j}^{12} D_{i-1,l} + \sum_{l=1}^{l} D_{i,j} & \text{if } j < 12 \\ X_{t,j}^{12} = \sum_{l=j-12+1}^{j} D_{i-1,l} & \text{if } j > 12 \end{cases} \tag{8}$$

$$F(\mathrm{X}) = \left[1 + \left(\frac{\partial}{X - \gamma}\right)^{\rho}\right]^{-1} \tag{9}$$

$$\mathrm{p} = 1 - F(\mathrm{x}) \tag{10}$$

$$w = \begin{cases} \sqrt{-2\ln p} & \text{if } p \le 0.5 \\ \sqrt{-2\ln(1-p)} & \text{if } p > 0.5 \end{cases} \tag{11}$$

$$SPEI = \frac{2.515517 + 0.802853w + 0.010328w^2}{1 + 1.432788w + 0.189269w^2 + 0.001308w^3} - w \tag{12}$$

where D_j is the difference between precipitation (P_j) and potential evapotranspiration (PET_j). PET_j is calculated by Thornwaite method due to the readily accessible parameters [38]. $X_{i,j}^{12}$ is the aggregated D_j at 12-month scale in the j^{th} month of the i^{th} year. The process of SPEI is the aggregation and normalization of D_j at 12-month scale according to Eqs. (8)-(11). α, β,and γ are the scale, shape and origin parameters, respectively. The normalization process is based on the log-logistic distribution. Positive SPEI value represents the wet condition, and a negative value indicates the dry condition [27], [39].

3) PRINCIPAL COMPONENTS ANALYSIS

Principal component analysis (PCA), a dimension reduction method, is used to classify the sub-regions of wetness / dryness based on SPEI values [40]. This method can extract structural information with homogeneous variance characteristics [29]. By calculating the covariance matrix with corresponding eigenvalues and eigenvectors, most of the total variances in the original data can be explained by some linear uncorrelated principal components (PCs) [32]. The normalized eigenvectors also called ''loadings'', represent the correlational relationship between the original data and the corresponding PCs, and refer to the weights of the original variables in the calculated PCs. The PCs need to check the adequacy of the samples through Bartlett's test p-value of sphericity and the Kaiser-Meyer-Olkin (KMO) test so that we can ensure the refined PCA calculation. The number of PCs depends on the proportion of the cumulative variance explained by the PCs. The hypothesis value is satisfactory in the rage of 60 - 70% and the extracted principal components should account for at least 5-10% of the data variance. In addition, to identify a more robust localized classification, the Varimax rotation method [41] is adopted in this study. This method is usually used for variance maximization of correlation coefficient (r^2) between the Rotated Principal Components (RPCs) and the variables, which simplifies the spatial patterns of parallel temporal disparities [27]. The Varimax rotation attempts to de-noise the column of loads so that each component is explained by a finite set of variables [39], [40], [43]. We found that the threshold value of RPCs from 0.5 to 0.6 was reasonable for spatial division of the sub-regions experiencing similar wetness / dryness changes during the study period [44], [45].

4) STATISTIC ANALYSIS

To provide an extensive explanation of climate change impacts on plant growth and the response of CPP to climate factors, the climate trend rate is used in this study. Climatic trend rate is computed using the following formula:

$$X = \mathrm{b}_0 + \mathrm{b}_1 t \quad (t = 1, 2, 3, \cdots n) \tag{13}$$

where X represents temperature, precipitation and CPP respectively, b_1 is the slope of linear regression trend. Since average temperature and total precipitation change little every year. The climatic trend rate of meteorological elements is expressed as 10 times of b_1 [46]. However, the change of carbon every year can be more than 100 g C/m^2/a. Consequently, the slope of CPP can be used the unit of ''g C/m^2/a^2'' [47].

Besides that, F test is used in this study to test the significance of the linear regression trend. The spatial distribution of correlation coefficients between CPP and temperature or precipitation is calculated using the following formula:

$$\mathrm{r_{xy}} = \frac{\sum_{i=1}^{n} (\mathrm{CPP}_i - \overline{CPP})(y_i - \bar{y})}{\sqrt{\sum_{i=1}^{n} (\mathrm{CPP}_i - \overline{CPP})^2 \sum_{i=1}^{n} (y_i - \bar{y})^2}} \tag{14}$$

where y_i is the climate factors, that is, precipitation (mm) and temperature (°C) in i^{th} year, and $\bar{y}$ is the mean values of climate factors over 39 years. If the correlation coefficients pass the significance test, then indicating that there exists an extremely significant ($p < 0.01$) or significant ($p < 0.05$) linear correlation. If r_{xy} is larger than zero, it means there exist a positive relationship between x and y variables, and vice versa.

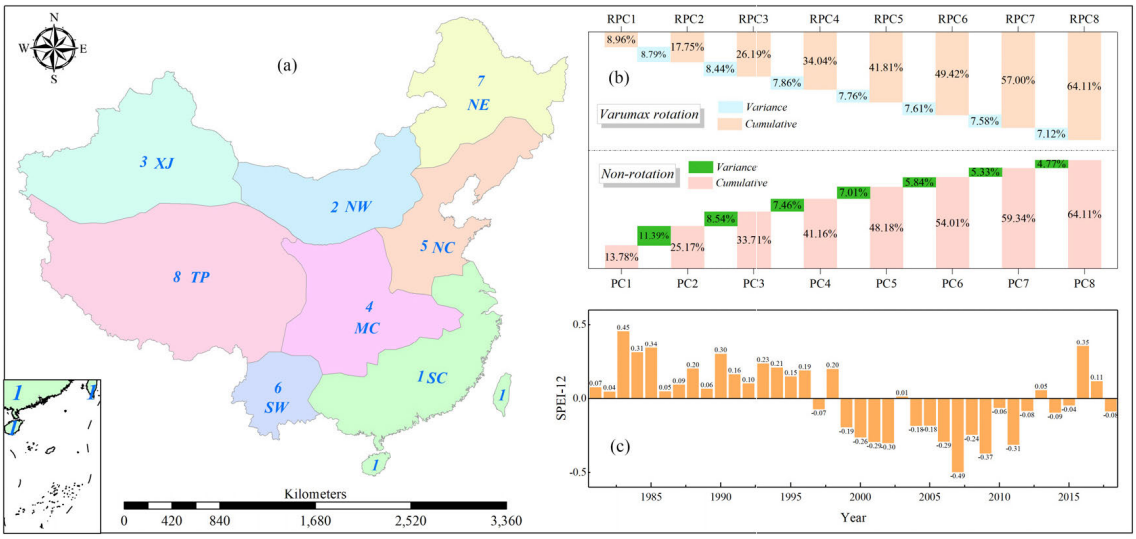

FIGURE 2. The eight different regions; (a) represents the 8 principal components according to RPCs loadings (Numbers 1-8), every sub-region is according to the ANUSPLIN (version 4.2) interpolation based on the RPCs loadings of every station. (b) is the different RPCs Loadings. Loading1 represents that this region is with a threshold value of RPCs loadings from 0.5-0.6 in the first principal component, and so on. (PC is a principal component with non-rotation. RPC is a principal component with Varimax rotation). (c) Average SPEI on 12-month scale in China.

5) VALIDATION

In order to validate the reliability and accuracy of the results, we also use the cross-experiment method to analyze the accuracy of the model in terms of data input, as well as the comparative analysis method with others' results, which provides a basis for further analysis of CPP and its spatio-temporal dynamic changes over China in last 39 years. We use the cross-experiment to compare with ANUSPLIN (version 4.2) and Kriging interpolation methods, respectively. 90% of the total number of stations are used to interpolation and 10% for validation. Additionally, we use a comparative analysis method to compare the estimated CPP of the synthetic model with current in-situ data and literatures.

III. RESULTS AND DISCUSSION

A. PCA REGIONALIZATION

In order to reveal the characteristics of CPP influenced by the climate factors at a sub-regional scale, the study area is divided into 8 sub-regions based on SPEI12 using the PCA and the Varimax rotation methods. The validation results show that the Bartlett's test p-value is very low (<0.001) and the KMO test is 0.60, meaning that the SPEI12 time series is well propitious for the PCA regionalization analysis. Eight principal components with a cumulative percentage of 64.11% are selected at station scales (Fig. 2b). The spatial patterns of these first eight components series are characterized by mapping the loading matrix. As shown in Fig. 2, the eight major regions includes Loading1, Southern China (SC); Loading 2, Northwestern China (NW); Loading 3, the Xinjiang (XJ); Loading 4, middle part of China (MC); Loading 5, Northern China (NC); Loading 6, Southwestern China (SW); Loading 7, Northeastern China (NE); Loading 8, Tibetan Plateau (TP).

B. TEMPORAL AND SPATIAL VARIABILITY OF CLIMATE FACTORS

1) TEMPORAL VARIABILITY OF CLIMATE FACTORS

Fig. 7 confirms that the increase in average temperature and decrease in annual precipitation are already evident over China during the last 39 years ($p<0.01$). However, various trends in climate change occur in different regions. Regions that show an opposite tendency variation of temperature and precipitation are mainly distributed in the MC, NC, NE and SW regions, as well as a certain degree of warming and drying phenomenon, especially in SW region (Table1). Similar increasing trends of temperature and precipitation are observed in other regions, such as XJ, NW, SC and TP. These climate change patterns are the determinant factors to affect the growth of terrestrial vegetation at different sub-regions.

2) SPATIAL VARIABILITY OF CLIMATE FACTORS

The spatial distribution of average annual temperature in China during 1980-2018 has obvious regional differences (Fig. 8a), showing a piecemeal increasing trend from northwest to southeast. The TP and NE are governed by relatively low temperatures, mainly due to the combined influence of altitude and latitude. The temperature in most regions of China shows a significant increasing trend, especially in the MC, SC and most areas of NW where the climate change rate can reach up to 0.2°C - 0.4°C/10a. However, the temperature in TP and northwest of NE has a slight decline during the study period. The total annual precipitation decreases gradually from the Southeast coast to the Northwest

TABLE 1. Characteristics of climate factors in different sub-regions from 1980 to 2018.

Region	SC	NW	XJ	MC	NC
Ave-Temperature (°C)	18.8	6.2	7.5	13.6	10.2
Climate trend rate (°C/10a)	0.3**	0.4**	0.2**	0.4**	0.3*
Precipitation (mm)	1599	253	186	1043	656
Climate trend rate (mm/10a)	1	0	6	-20	-10
Region	SW	NE	TP	The National Scale	
Ave-Temperature (°C)	16.0	1.4	-0.1	8.2	
Climate trend rate (°C/10a)	0.5**	0.3**	0.4**	0.4**	
Precipitation (mm)	1201	499	212	786	
Climate trend rate (mm/10a)	-40**	-9	0	-21**	

Note: ** represents a test with a significance level of 0.01, * represents a test with a significance level of 0.05. The underline words represent that there is an opposite variation tendency of temperature and precipitation in these regions, which would lead to a certain degree of warming and drying phenomenon.

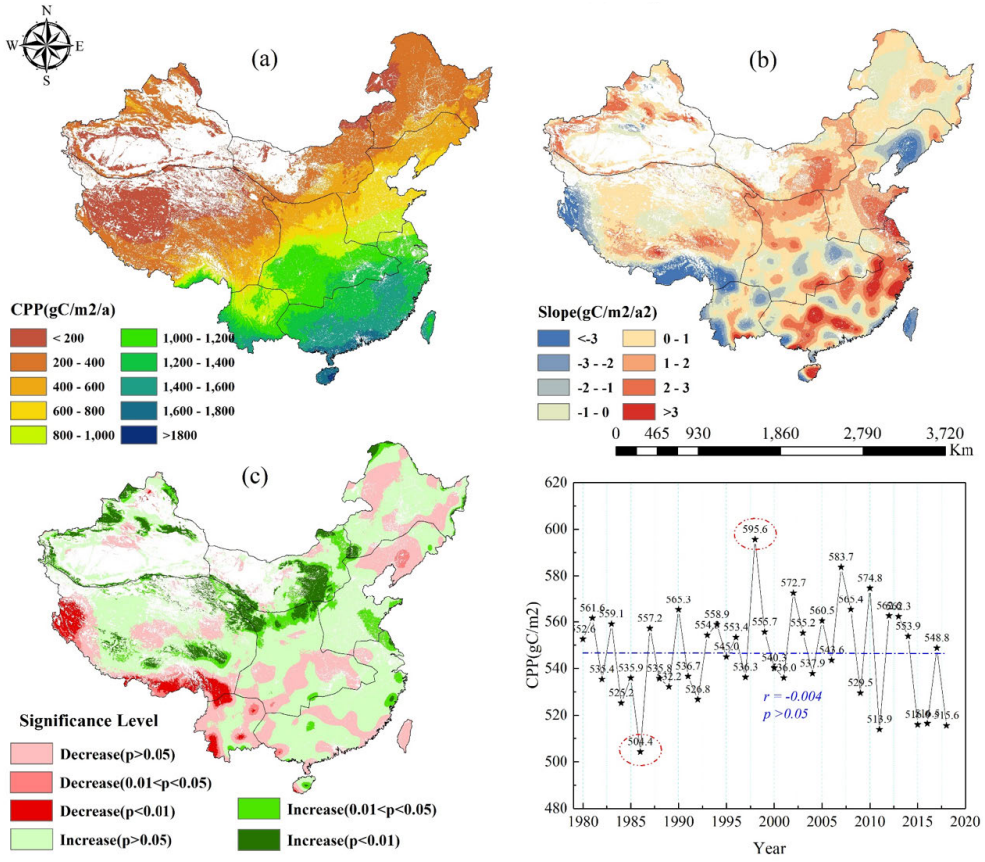

FIGURE 3. (a) Spatial distribution of annual CPP, (b) the variation tendency of vegetation CPP, and (c) the significant level in the study area from 1980 to 2018. (d) Annual variation of CPP from 1980 to 2018.

inland (Fig. 8d). The average annual precipitation in the South and Southeast Coastal areas of the Yangtze River is generally over 1300 mm, mainly due to the monsoon climate. Fig. 8e & f show that China's annual precipitation trends present spatially patchy variation from 1980 to 2018. Nationwide, there is a little change in precipitation with a rate of -12mm/10a, and most regions of China show an insignificantly decreased tendency except for some part of the TP and SW. Additionally, the mild increase appears in the region of north TP and northwest of NE during the study period.

C. TEMPORAL AND SPATIAL VARIABILITY OF CPP

1) TEMPORAL VARIABILITY OF CPP

In the last 39 years, the CPP of vegetation in China presents highly fluctuated. The average annual CPP of veg-

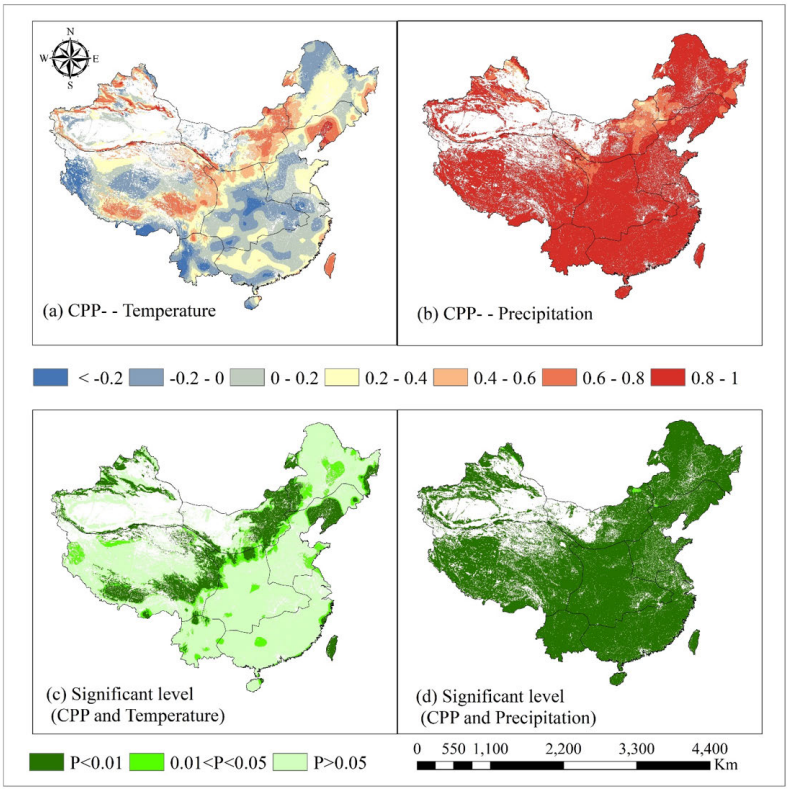

FIGURE 4. Spatial distribution of correlation coefficient (a, b) and significant level (c, d) of CPP and climate factors.

etation in the past 39 years is 546.58 g C · m^{-2} · a^{-1} at the national scale. The minimum and maximum values appear in 1986 (504.35g C · m^{-2}· a^{-1}) and 1998 (595.60 g C · m^{-2} · a^{-1}), respectively (Fig. 3d). Accordingly, we validate the trend of 1980-1986, 1986-1998 and 1998-2018. A significant decreasing level is found during 1998 to 2018 ($r = -0.45$, $p<0.05$), while insignificant trends appear during 1980-1986 and 1986-1998. A noticeable increase of CPP in 1998 because La Niña events caused a significant increase in precipitation [48]–[50].

2) SPATIAL VARIABILITY OF CPP

As is shown in Fig. 3a, CPP distribution differs among different zones, showing a gradually increasing trend from northwest to southeast. Annual vegetation CPP as usually higher than 600 g C · m^{-2} · a^{-1} appears in SC region, where productive evergreens are widely distributed with abundant precipitation, warm climate, and abundant groundwater [51]. Annual CPP in Northwest of China such as most areas of the NW, NE, TP and XJ is lower than 200 g C · m^{-2} · a^{-1}, where the climate is dominated by a relatively lower temperature and less rainfall than other regions [52]. Overall, the maximum values of CPP during a 39-year period (1980-2018), appear in the southwest, southern China, and Taiwan regions. High CPP is found mainly in areas, i.e., the southern tropical humid regions and the southeastern margin of the Yangtze River, Yunnan-Guizhou Plateau, and north of Nanling Mountains with annual CPP more than 800 g C · m^{-2} · a^{-1}. Likewise, the median CPP values with annual average CPP between 500 and 800 g C · m^{-2} · a^{-1} are found mainly in areas with crops harvested two or three times every year, or three harvest times every two years [53], e. g., middle reaches of the Yangtze River Basin, most regions of Sichuan, southeastern Tibet, and Huang-Huai-Hai Plain. The low-value areas mainly distribute in Inner Mongolia, Xinjiang, Tibetan Plateau, Gansu, and Ningxia provinces with annual CPP between 200 and 400 g C · m^{-2} · a^{-1}, primarily in grassland and one season or two seasons crops or arid crops with less water availability [53]. Fig. 3b & c show that a significant CPP increase and positive vegetation growth response appear in some parts of China, such as the most area of NW and some part of XJ ($p < 0.01$). The CPP loses mainly occur in some regions of the TP and SW, while the decreases in other regions are not significant ($p > 0.05$).

D. RESPONSE CHARACTERISTICS OF CPP TO CLIMATE CHANGE

1) RESPONSE CHARACTERISTICS IN DIFFERENT SUB-REGIONS

Fig. 4 illustrates the positive correlation between CPP and precipitation predominated in the whole area ($p < 0.01$). The average correlation coefficients can reach 0.92 at national

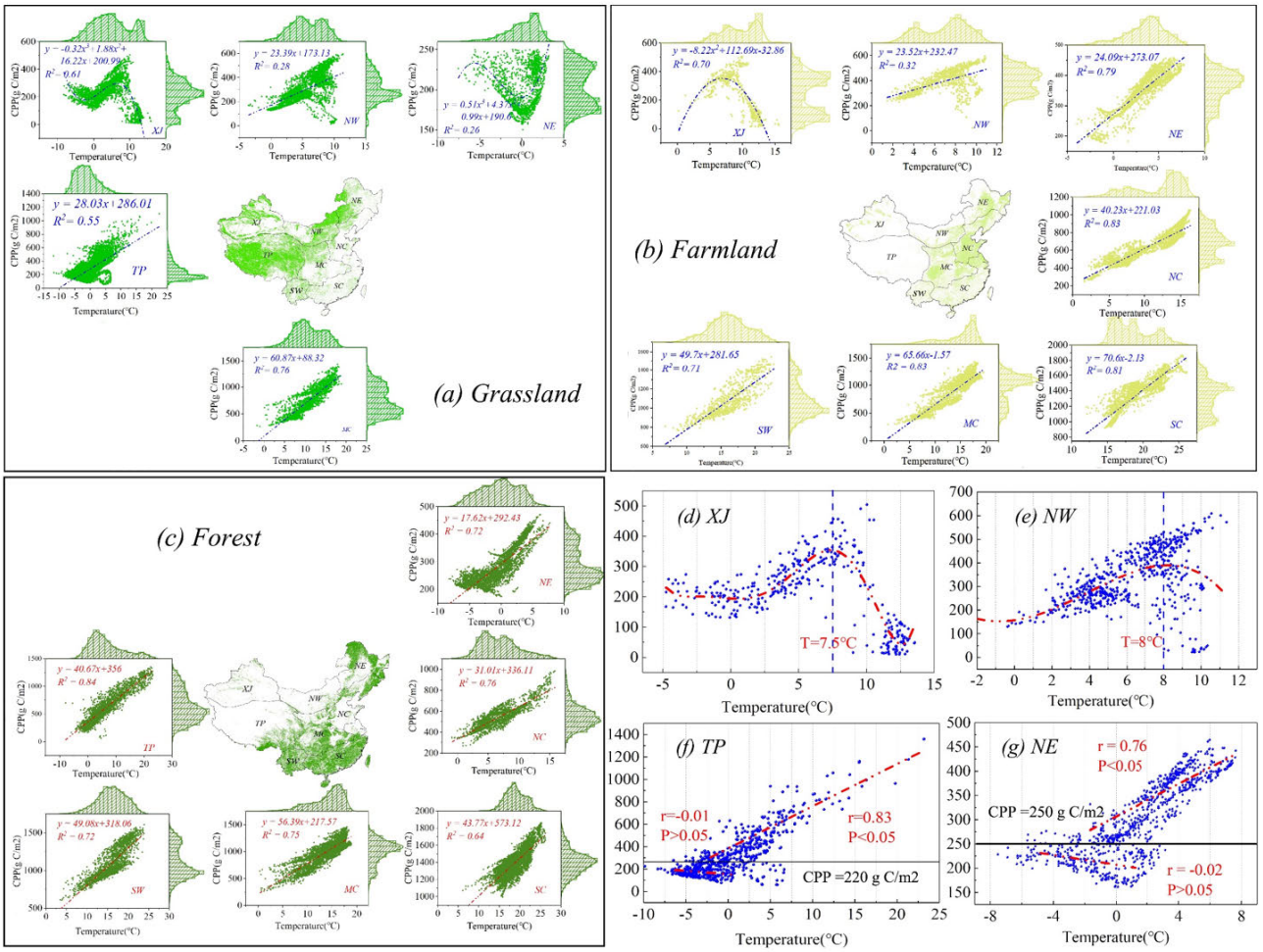

FIGURE 5. The relationships between annual CPP and annual temperature at different sub-regions of vegetation ecosystems over China (a. grassland ecosystem, b. farmland ecosystem and c. forest ecosystem). Mainly sub-region distributions of each ecosystem are shown in FIGURE a, b and c. FIGURE d-g represent the responses of CPP to temperature in four special sub-regions with significant level (1000 grid cells are selected for correlation analysis at each region).

scale. Only the NW region has average correlation coefficients (r = 0.78) lower than that of any other regions. Moreover, some arid regions with increasing vegetation growth responses indicate that the precipitation is helpful to the growth of vegetation in drought areas, especially in the most area of NW and some part of XJ. In contrast, the temperature response to vegetation CPP has obvious spatial heterogeneity. Regions displaying an insignificant negative correlation are mainly distributed in NC, MC, SW, and SC regions (Fig. 4a & c). Only in the regions of NW, XJ, northern NC, and the eastern and south fringe of TP, significant positive correlations are observed, indicating that warmer temperatures can promote the increase of vegetation CPP in these regions.

Overall, precipitation is the predominant factor controlling the spatial distribution of CPP, especially in the semi-arid regions in North China, which is in good accordance with others' studies based on the field observations [54]. Temperature variations may have a significant impact on the CPP at a regional scale [55], such as TP and NE regions with high-altitude or high-latitude, where ecosystems are more vulnerable and more sensitive to climate change.

2) RESPONSE CHARACTERISTICS IN DIFFERENT ECOSYSTEMS

Fig. 5a illustrates that grassland in China mainly distributes in XJ, NW, NE, and TP regions. A low linear correlation between CPP of grassland ecosystem and temperature occur in NW and intricate correlations in XJ and NE. CPP shows a decreasing tread when the average temperature is greater than 7.5°C. In a country scale, the CPP of the grassland ecosystem mostly concentrates on 200-500 g C/m^2/a where CPP accounts for 81.6 % of the total amounts and the corresponding temperature is between −10°C and 10°C. CPP shows an insignificant decreasing trend with the increase of temperature in this temperature range ($r = -0.07$, $p > 0.05$). When the annual average temperature is higher than 10°C, the grassland CPP increases significantly with the increase

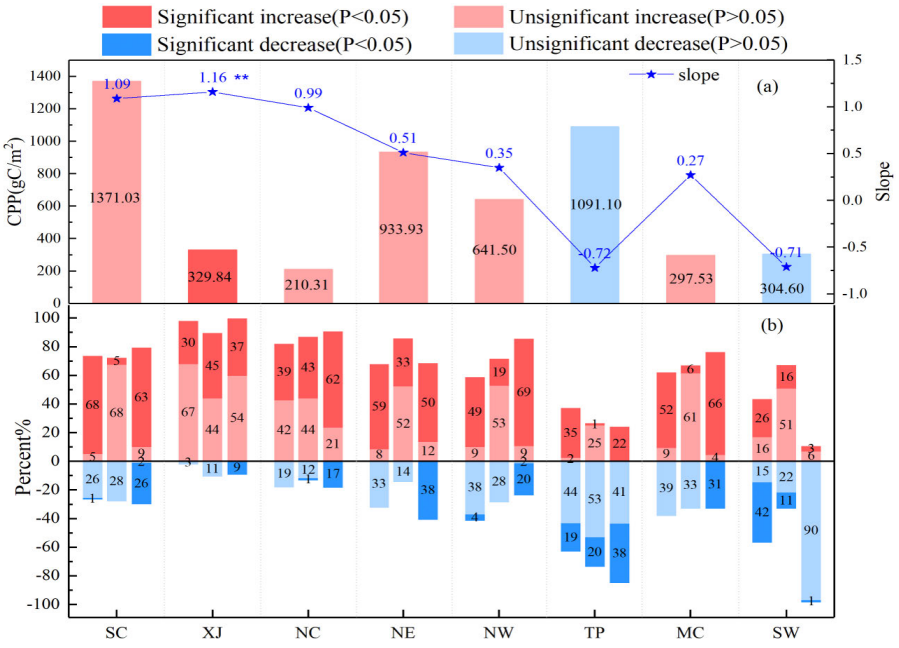

FIGURE 6. (a) The average vegetation CPP of different regions and the average change rate. Different colors of column represent the different significances and ** indicates the slope passed the 0.05 significance test. (b) The proportion of significant variation of vegetation CPP in different regions. The column from left to right is, forest, grassland and farmland. Different colors of column represent the different significances.

of temperature. However, the frequency (18.4%) of CPP of grassland ecosystem in this temperature range is less than that in the range of -10 −10°C. Therefore, the results also demonstrate that the grassland vegetation ecosystem is restrained by the rising trend of temperature in most regions. In terms of farmlands, the CPP is found to be a significant positive linear correlation with temperature except for XJ where CPP shows a decreasing tread when temperature is greater than 7.5°C (Fig. 5b). A slight decrease is observed in NW when the average temperature is higher than 6.2°C. Spatially, these regions are located in the arid regions where crop growth is restricted by the drought. Fig. 5c illustrates that forest in China mainly distributes in NE, SW, SC, and MC, where the linear positive correlations between CPP and temperature appear in each sub-region, especially in TP, NE and northeast of NC with high-altitude or high-latitude.

The above results show that the relationship of ecosystem CPP and temperature has high regional differences, especially in XJ, NW, NE and TP regions. Consequently, random sample selection is carried out in the four regions with significant correlations, and 1000 grid cells are selected for correlation analysis in each region. Fig. 5d & e show that the effect of temperature on vegetation CPP increases first and then decreases with the increase of temperature in XJ and NW. The optimum temperatures for vegetation in the two regions are 7.5°C and 8°C, respectively. When the average annual temperature in these two regions is lower than the optimum temperature, the CPP of vegetation increases with the increase of temperature, and vice versa. These two regions are mainly concentrated in the arid areas of Western China, where the annual temperature is 7.5°C and 6.2°C, respectively (Table 1). Thus, the current temperature in XJ and NW is suitable for vegetation growth. The CPP of vegetation is lower than 250 g C/m^2 in TP and NE regions (Fig. 5f & g) with an average annual temperature lower than 0°C, where the temperature has no significant influence on CPP change. However, the annual average temperature is - 0.1°C and 1.4°C in these two regions, and the climate change rate increases by 0.3°C and 0.5°C per decade, respectively, which can conclude that the rise in temperature has no significant positive effects on the overall change of vegetation for the moment.

IV. DISCUSSION

A. DISCUSSION ABOUT THE RELIABILITY OF THE SYNTHETIC MODEL

Because of the uneven distribution of meteorological stations, there may be some uncertainties during the interpolation process. In addition, the interpolation method is also a weakness in detecting mutation rather than gradual heterogeneity in data [35]. The cross-experiment method is used to analyze the accuracy of the model in terms of data input. Fig. 9 shows that the interpolation results of input data have a good consistent with the validation results, especially for the Anusplin interpolation method with a high correlation (R^2_{temp} = 0.85, R^2_{prec} = 0.95). Herewith, we choose the Anusplin interpolation method to process the input data in this study because this method takes into account the DEM information.

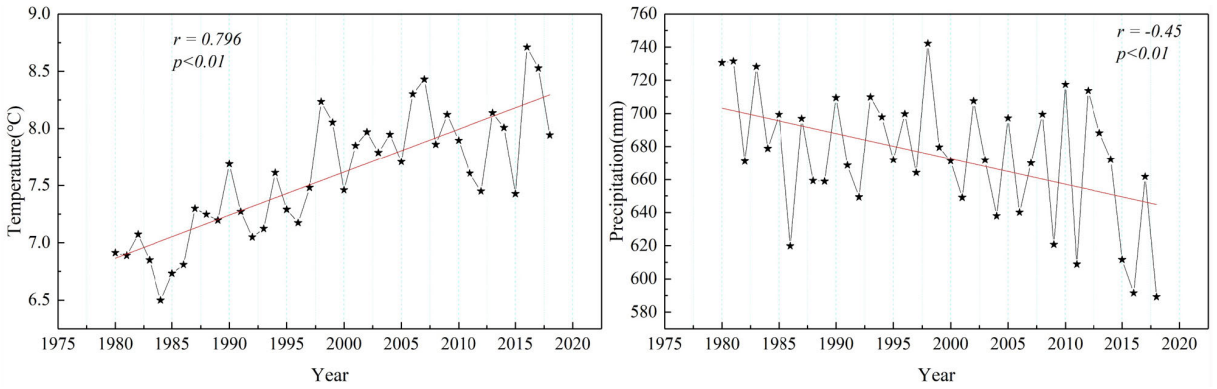

FIGURE 7. Annual variation of the precipitation (a) and temperature (b).

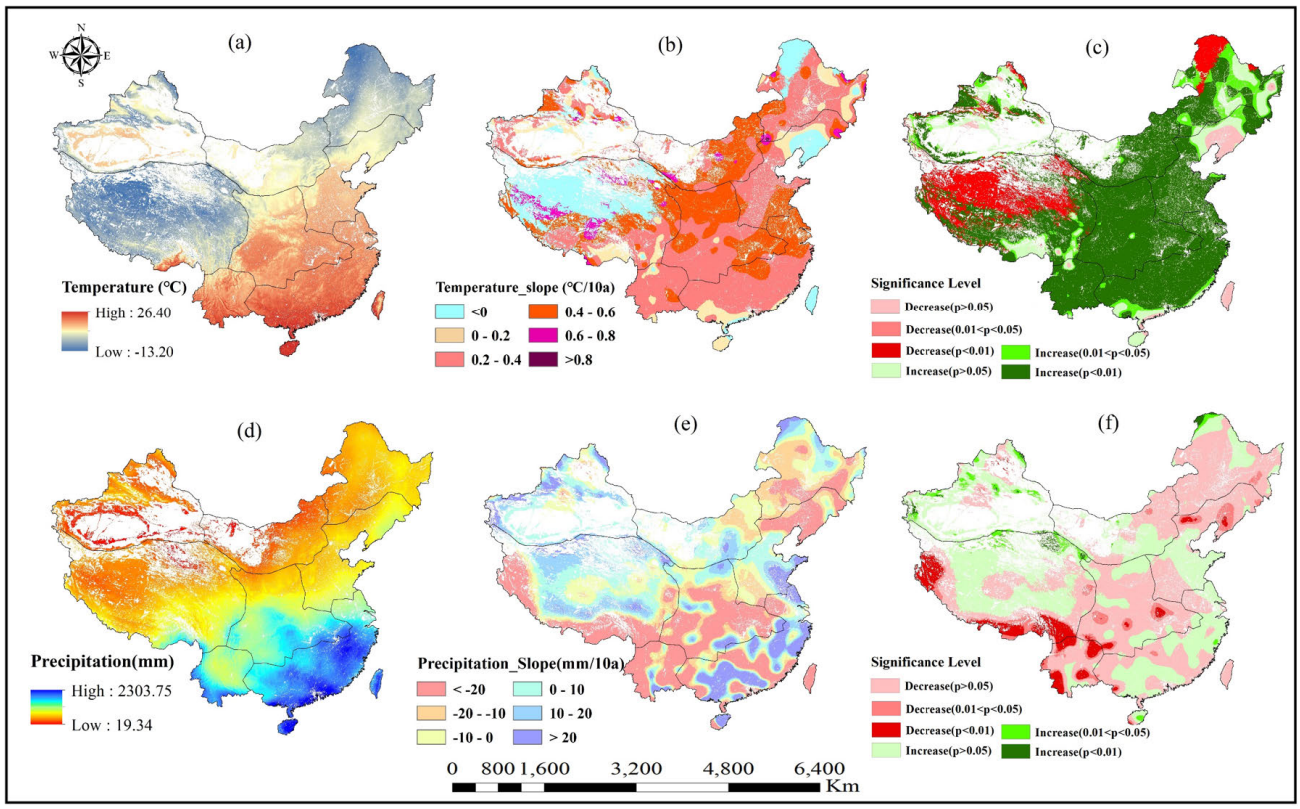

FIGURE 8. (a) Spatial distribution of annual average temperature, (b) climate tendency rate of temperature, and (c) the significant level of temperature. (d) Spatial distribution of annual mean precipitation, (e) climate tendency rate of precipitation, and (f) the significant level of precipitation.

These results not only guarantee the accuracy of the input data but also provide a basis for the follow-up research results.

Additionally, we use a comparative analysis method to compare the estimated CPP of the synthetic model with current observed data and literatures. Only two observed NPP stations are collected in China (Fig. 1 and Table 2). The results show that the error between the measured data and the simulated value in this study is larger in Ulanhot than in Xilinhot. This may be due to the CPP in our study shows the maximized NPP. The total CPP of China simulated in our study is 2.47Pg C (1Pg C = 10^{15} g C). This is within the range of published experiments of 1.95-6.13 Pg C [35], [52], [56], [57]. Therefore, the synthetic model can assess the potential productivity of terrestrial ecosystems.

B. DISCUSSION ABOUT THE SIGNIFICANT OF CPP RESPONSES TO CLIMATE CHANGE

The potential trends and significant variation levels of three vegetation ecosystems in various regions are different. Fig. 6 shows a slight increasing trend of CPP (slope = 0.19 g C · m^{-2} · a^{-2}, $p>0.05$) in a national scale.

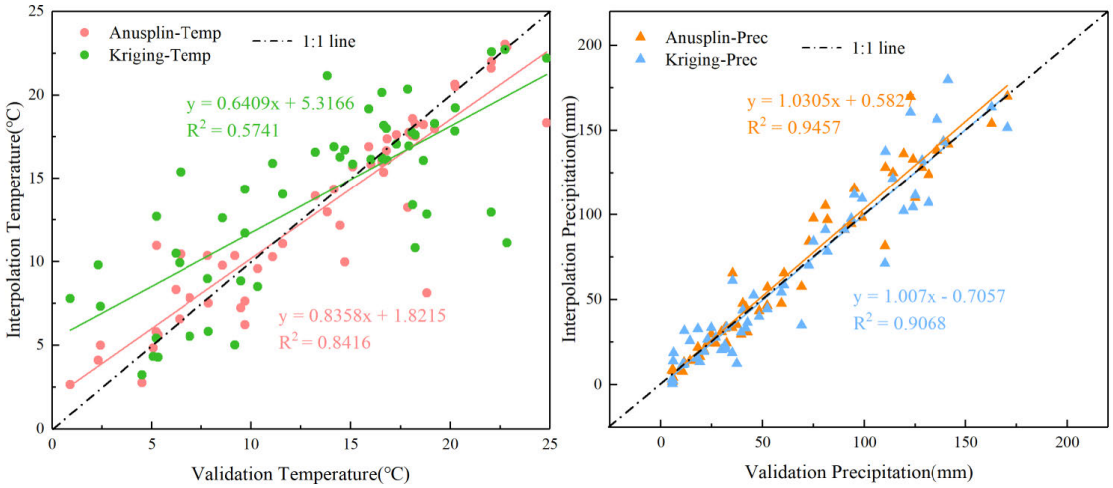

FIGURE 9. Validation of interpolation methods. Temp is the abbreviation of Temperature and Prec is the abbreviation of Precipitation.

TABLE 2. Validation of simulated CPP compared with observation data.

City	Region	Vegetation type	ANPP (g C·m^{-2}·a^{-1})	Observed date	ANPP in this study
Ulan Hot	Xing'an League	grassland	152	1981-1990	
Ulan Hot	Xing'an League	grassland	152	1981-1990	384.64
Ulan Hot	Xing'an League	grassland	162	1981-1990	
Xilinhot	Xilingol League	grassland	248.63	1980-1989	237.7

** ANPP means above net primary productivity. The calculated results of CPP in this study is ANPP.

However, the slope of the CPP and the significance test both demonstrate that the changes in vegetation ecosystems are heterogeneous. An increasing trend toward CPP and positive vegetation growth responses are shown in SC, XJ, NC and NE regions, especially XJ (slope $= 1.16$ g C $\cdot$ m^{-2} $\cdot$ a^{-2}, $p<0.05$) (Fig. 6a). Meanwhile, an insignificant decreasing trend occurs in the region of TP, MC and SW. The significant increase of forest CPP in different regions is relatively greater than grassland and farmland ecosystems. Specifically, the proportion of increasing trends of CPP is greater than that of decreasing in SC, XJ, NC, NE, NW, and MC regions. This could be closely related to the implementation of a series of national-level ecological projects and policies in the central and western regions of China in the late 1990s and early 2000s [58]. For example, the Grazing Withdrawal Program (GWP) launched in 2003, particularly emphasized on relieving grazing pressure and reestablishing the degenerative land through appropriate grazing, planting trees and grassland, or other suggestions and measurements in the western and central regions of China [5]. Whereas, as shown in Fig. 6b, the proportion of decreasing trends is greater than that of increasing in TP due to the worse environmental conditions. The same relationships are also observed at farmland and forest CPP in SW, which is consistent with Shang's study [53]. The presumed main reason for these phenomena is that the decrease of the average annual precipitation may also lead to a decrease in CPP.

C. UNCERTAINTIES

In this study, CPP represents the vegetation can make full use of climate resources. However, vegetation CPP is influenced by different climate factors, such as CO_2, radiation, and wind speed, etc. The synthesis model takes less factors into account and is relatively simple. There are large uncertainties because the real situation is not entirely the same as the simulation. Many studies have reported that spatial-temporal variations are obvious among different vegetation types, e. g., forest, grassland, and farmland ecosystems [37], [53], [56], [59]. Additionally, the limitation of the spatial resolution of remote sensing image data, a large number of mixed pixels are generated in the image, which affects the simulation results of CPP. As for the multi-year CPP average, the uncertainty in simulated CPP is also resulted from climate input data such as the differences in temperature, precipitation, topography and other aspects at the station scale through interpolated tools. These deficiencies may address in future works. However, the reports have indicated that this method has better advantages in various regions [5], [15], [46]. The accuracy of the extraction results is acceptable. Accordingly, our study provides new insight into the large-scale and long-time series CPP evaluation.

V. CONCLUSION

This study used the synthetic method and statistical analysis to evaluate the spatial and temporal distribution of CPP in different terrestrial ecosystems and different sub-regions over China from 1980 to 2018. Meanwhile, we analyzed the responses of CPP in different sub-regions to the climate parameters, i.e., temperature and precipitation. The CPP of terrestrial vegetation shows a gradually increasing trend from northwest to southeast of China. The overall tendency of CPP presents a slightly increasing trend over recent 39 years, with

an increased rate of 0.19 g C · m^{-2} · a^{-2}. The climatic trend rate in annual average precipitation and temperature are −21 mm/10a and 0.4 °C/10a, respectively. The positive correlation between CPP and precipitation is more obvious than that of temperature, indicating that precipitation is the most important climatic factor determining the productivities of vegetation in the whole country. The optimum temperature for CPP in XJ and NW is 7.5°C and 8°C, respectively. Additionally, grassland CPP shows complex trends in XJ, SW, NE and TP regions, especially in XJ, a CPP-decreasing trend when the temperature is more than 7.5°C, whereas in NE, an increasing trend when the temperature is more than 0°C. Linear correlations are shown between farmland CPP and temperature in each sub-region except for XJ. The similar relationships also appear on forest CPP, especially in TP, NE and northeast of NC with high-altitude or high-latitude. However, under the trend of increasing temperature and decreasing precipitation, there are negative effects on the CPP of vegetation over China, whether in some sub-regions or different ecosystems, indicating that drier and warmer weathers are detrimental for vegetation growth.

APPENDIX

See Figs. 7–9.

REFERENCES

[1] Y. Zhang, C. Zhang, Z. Wang, Y. Chen, C. Gang, R. An, and J. Li, "Vegetation dynamics and its driving forces from climate change and human activities in the three–river source region, China from 1982 to 2012," *Sci. Total Environ.*, vols. 563–564, pp. 210–220, Sep. 2016.

[2] Y. Gao, X. Zhou, Q. Wang, C. Wang, Z. Zhan, L. Chen, J. Yan, and R. Qu, "Vegetation net primary productivity and its response to climate change during 2001–2008 in the Tibetan Plateau," *Sci. Total Environ.*, vol. 444, pp. 356–362, Feb. 2013.

[3] F. Chen, A. Lin, H. Zhu, and J. Niu, "Quantifying climate change and ecological responses within the yangtze river basin, China," *Sustainability*, vol. 10, no. 9, p. 3026, Aug. 2018.

[4] D. Wu, X. Zhao, S. Liang, T. Zhou, K. Huang, B. Tang, and W. Zhao, "Time-lag effects of global vegetation responses to climate change," *Glob Change Biol.*, vol. 21, no. 9, pp. 3520–3531, Sep. 2015.

[5] C. Gang, W. Zhao, T. Zhao, Y. Zhang, X. Gao, and Z. Wen, "The impacts of land conversion and management measures on the grassland net primary productivity over the Loess Plateau, Northern China," *Sci. Total Environ.*, vol. 645, pp. 827–836, Dec. 2018.

[6] W. Zhou, C. Gang, L. Zhou, Y. Chen, J. Li, W. Ju, and I. Odeh, "Dynamic of grassland vegetation degradation and its quantitative assessment in the northwest China," *Acta Oecol.*, vol. 55, pp. 86–96, Feb. 2014.

[7] R. Wang and J. A. Gamon, "Remote sensing of terrestrial plant biodiversity," *Remote Sens. Environ.*, vol. 231, Sep. 2019, Art. no. 111218.

[8] T. Chen, A. Bao, G. Jiapaer, H. Guo, G. Zheng, L. Jiang, C. Chang, and L. Tuerhanjiang, "Disentangling the relative impacts of climate change and human activities on arid and semiarid grasslands in central Asia during 1982–2015," *Sci. Total Environ.*, vol. 653, pp. 1311–1325, Feb. 2019.

[9] J. W. Raich, E. B. Rastetter, J. M. Melillo, D. W. Kicklighter, P. A. Steudler, B. J. Peterson, A. L. Grace, B. Moore, III, and C. J. Vorosmarty, "Potential net primary productivity in South America: Application of a global model," *Ecol. Appl.*, vol. 1, no. 4, pp. 399–429, 2013.

[10] R. Misra, *Primary Productivity of the Biosphere*. New York, NY, USA: Springer-Verlag, 1975.

[11] X.-C. Ye, Y.-K. Meng, L.-G. Xu, and C.-Y. Xu, "Net primary productivity dynamics and associated hydrological driving factors in the floodplain wetland of China's largest freshwater lake," *Sci. Total Environ.*, vol. 659, pp. 302–313, Apr. 2019.

[12] S. Wu, S. Zhou, D. Chen, Z. Wei, L. Dai, and X. Li, "Determining the contributions of urbanisation and climate change to NPP variations over the last decade in the Yangtze River Delta, China," *Sci. Total Environ.*, vol. 472, pp. 397–406, Feb. 2014.

[13] Y. Liu, Y. Yang, Q. Wang, X. Du, J. Li, C. Gang, W. Zhou, and Z. Wang, "Evaluating the responses of net primary productivity and carbon use efficiency of global grassland to climate variability along an aridity gradient," *Sci. Total Environ.*, vol. 652, pp. 671–682, Feb. 2019.

[14] H. Yan, L. Pan, Z. Xue, L. Zhen, X. Bai, Y. Hu, and H.-Q. Huang, "Agent-based modeling of sustainable ecological consumption for grasslands: A case study of inner Mongolia, China," *Sustainability*, vol. 11, no. 8, p. 2261, Apr. 2019.

[15] C. Gang, Y. Zhang, Z. Wang, Y. Chen, Y. Yang, J. Li, J. Cheng, J. Qi, and I. Odeh, "Modeling the dynamics of distribution, extent, and NPP of global terrestrial ecosystems in response to future climate change," *Global Planet. Change*, vol. 148, pp. 153–165, Jan. 2017.

[16] M. Zhang, R. Lal, Y. Zhao, W. Jiang, and Q. Chen, "Estimating net primary production of natural grassland and its spatio-temporal distribution in China," *Sci. Total Environ.*, vol. 553, pp. 184–195, May 2016.

[17] Z. J. Li, C. C. Duan, L. L. Jin, X. Q. Hu, B. Li, and H. Y. Yang, "Spatial and temporal variability of climatic potential productivity in Yunnan Province, China," (in Chinese), *Chin. J. Appl. Ecol.*, vol. 30, no. 7, pp. 2181–2190, 2019.

[18] L. Li, H. F. Zhou, and A. M. Bao, "Spatial and temporal variability of potential climate productivity in central Asia," (in Chinese), *J. Resour., Natural*, vol. 29, no. 2, pp. 285–294, 2014.

[19] J. Guo, J. Zhao, Y. Xu, Z. Chu, J. Mu, and Q. Zhao, "Effects of adjusting cropping systems on utilization efficiency of climatic resources in Northeast China under future climate scenarios," *Phys. Chem. Earth*, vols. 87–88, pp. 87–96, Jan. 2015.

[20] A. Zhou, "Preliminary study on the net primary productivity model of natural vegetation," *J. Plant Ecol.*, vol. 19, no. 3, pp. 193–200, 1995.

[21] S. W. Running and E. R. Hunt, *Generalization of a Forest Ecosystem Process Model for Other Biomes, BIOME-BGC, and an Application for Global-Scale Models*. Sawston, U.K.: Woodhead Publishing Limited, 1993.

[22] C. S. Potter, J. T. Randerson, C. B. Field, P. A. Matson, P. M. Vitousek, H. A. Mooney, and S. A. Klooster, "Terrestrial ecosystem production: A process model based on global satellite and surface data," *Global Biogeochem. Cycles*, vol. 7, no. 4, pp. 811–841, Dec. 1993.

[23] Q. Zhu, J. Zhao, Z. Zhu, H. Zhang, Z. Zhang, X. Guo, Y. Bi, and L. Sun, "Remotely sensed estimation of net primary productivity (NPP) and its spatial and temporal variations in the greater Khingan Mountain Region, China," *Sustainability*, vol. 9, no. 7, p. 1213, Jul. 2017.

[24] Q. Sun, C. Miao, and Q. Duan, "Extreme climate events and agricultural climate indices in China: CMIP5 model evaluation and projections," *Int. J. Climatol.*, vol. 36, no. 1, pp. 43–61, Jan. 2016.

[25] Y. Guo, S. Huang, Q. Huang, H. Wang, W. Fang, Y. Yang, and L. Wang, "Assessing socioeconomic drought based on an improved multivariate standardized reliability and resilience index," *J. Hydrol.*, vol. 568, pp. 904–918, Jan. 2019.

[26] Q. Zhou, Y. Luo, X. Zhou, M. Cai, and C. Zhao, "Response of vegetation to water balance conditions at different time scales across the karst area of southwestern China—A remote sensing approach," *Sci. Total Environ.*, vol. 645, pp. 460–470, Dec. 2018.

[27] H. Guo, A. Bao, T. Liu, G. Jiapaer, F. Ndayisaba, and L. Jiang, "Spatial and temporal characteristics of droughts in Central Asia during 1966–2015," *Sci. Total Environ.*, vol. 624, pp. 1523–1538, May 2018.

[28] S. Tong, Q. Lai, J. Zhang, Y. Bao, A. Lusi, Q. Ma, X. Li, and F. Zhang, "Spatiotemporal drought variability on the Mongolian Plateau from 1980–2014 based on the SPEI–PM, intensity analysis and Hurst exponent," *Sci. Total Environ.*, vol. 615, pp. 1557–1565, Feb. 2018.

[29] I. Bordi, K. Fraedrich, J.-M. Jiang, and A. Sutera, "Spatio-temporal variability of dry and wet periods in eastern China," *Theor. Appl. Climatol.*, vol. 79, nos. 1–2, pp. 81–91, Oct. 2004.

[30] Q. Wang, P. Shi, T. Lei, G. Geng, J. Liu, X. Mo, X. Li, H. Zhou, and J. Wu, "The alleviating trend of drought in the Huang-Huai-Hai Plain of China based on the daily SPEI," *Int. J. Climatol.*, vol. 35, no. 13, pp. 3760–3769, Nov. 2015.

[31] Z. Liu, Y. Wang, M. Shao, X. Jia, and X. Li, "Spatiotemporal analysis of multiscalar drought characteristics across the Loess Plateau of China," *J. Hydrol.*, vol. 534, pp. 281–299, Mar. 2016.

[32] T. Raziei, B. Saghafian, A. A. Paulo, L. S. Pereira, and I. Bordi, "Spatial patterns and temporal variability of drought in Western Iran," *Water Resour. Manage.*, vol. 23, no. 3, pp. 439–455, Feb. 2009.
[33] H. Guo, S. Chen, A. Bao, A. Behrangi, Y. Hong, F. Ndayisaba, J. Hu, and P. M. Stepanian, "Early assessment of integrated multi-satellite retrievals for global precipitation measurement over China," *Atmosp. Res.*, vols. 176–177, pp. 121–133, Jul. 2016.
[34] Y. Ding, S. Liang, and S. Peng, "Climate change affects forest productivity in a typical climate transition region of China," *Sustainability*, vol. 11, no. 10, p. 2856, May 2019.
[35] C. Gang, W. Zhou, J. Li, Y. Chen, S. Mu, J. Ren, J. Chen, and P. Y. Groisman, "Assessing the spatiotemporal variation in distribution, extent and NPP of terrestrial ecosystems in response to climate change from 1911 to 2000," *PLoS ONE*, vol. 8, no. 11, 2013, Art. no. e80394.
[36] X. Zhang, "The potential evapotranspiration (PE) index for vegetation and vegetation-climatic classification (1)—An introduction of main methods and PEP program," *J. Plant Ecol.*, vol. 13, no. 1, pp. 197–207, 1989.
[37] E. Q. Zhu, Y. Z. Pan, and J. S. Zhang, "Remote sensing estimation of net primary productivity of terrestrial vegetation in China," *J. Plant Ecol.*, vol. 31, no. 3, pp. 413–424, 2007.
[38] A. R. Pereira and W. O. Pruitt, "Adaptation of the thornthwaite scheme for estimating daily reference evapotranspiration," *Agricult. Water Manage.*, vol. 66, no. 3, pp. 251–257, May 2004.
[39] S. M. Vicente-Serrano, S. Beguería, J. I. López-Moreno, M. Angulo, and A. El Kenawy, "A new global 0.5° gridded dataset (1901–2006) of a multiscalar drought index: Comparison with current drought index datasets based on the palmer drought severity index," *J. Hydrometeor.*, vol. 11, no. 4, pp. 1033–1043, Aug. 2010.
[40] F. Santos, I. Pulido-calvo, and M. M. Portela, "Spatial and temporal variability of droughts in Portugal," *Water Resour. Res.*, vol. 46, pp. 1–13, Mar. 2010.
[41] M. B. Richman, "Rotation of principal components," *Int. J. Climatol.*, vol. 6, no. 3, pp. 293–335, 1986.
[42] J. Huang, S. Sun, Y. Xue, J. Li, and J. Zhang, "Spatial and temporal variability of precipitation and dryness/wetness during 1961–2008 in Sichuan province, West China," *Water Resour. Manage.*, vol. 28, no. 6, pp. 1655–1670, Apr. 2014.
[43] M. M. Portela, M. Zelenáková, J. F. Santos, P. Purcz, A. T. Silva, and H. Hlavatá, "Comprehensive characterization of droughts in Slovakia," *Int. J. Environ. Sci. Develop.*, vol. 8, no. 1, pp. 25–29, Sep. 2016.
[44] Y. Wang, T. Zhang, X. Chen, J. Li, and P. Feng, "Spatial and temporal characteristics of droughts in Luanhe River basin, China," *Theor. Appl. Climatol.*, vol. 131, nos. 3–4, pp. 1369–1385, Feb. 2018.
[45] T. Raziei, I. Bordi, and L. S. Pereira, "Regional drought modes in iran using the SPI: The effect of time scale and spatial resolution," *Water Resour. Manage.*, vol. 27, no. 6, pp. 1661–1674, Apr. 2013.
[46] C. Gang, W. Zhou, Z. Wang, Y. Chen, J. Li, J. Chen, J. Qi, I. Odeh, and P. Y. Groisman, "Comparative assessment of grassland NPP dynamics in response to climate change in China, North America, Europe and Australia from 1981 to 2010," *J. Agronomy Crop Sci.*, vol. 201, no. 1, pp. 57–68, Feb. 2015.
[47] C. Jiang and Y. Ryu, "Multi-scale evaluation of global gross primary productivity and evapotranspiration products derived from Breathing Earth System Simulator (BESS)," *Remote Sens. Environ.*, vol. 186, pp. 528–547, Dec. 2016.
[48] K. Wolter and M. S. Timlin, "Measuring the strength of ENSO events: How does 1997/98 rank?" *Weather*, vol. 53, no. 9, pp. 315–324, 1998.
[49] C.Hong-Ying, "Intensities and time-frequency variability of ENSO in the last years," (in Chinese), *J. Tropical Meteorol.*, vol. 33, pp. 683–694, Oct. 2017
[50] S. Piao, X. Zhang, A. Chen, Q. Liu, X. Lian, X. Wang, S. Peng, and X. Wu, "The impacts of climate extremes on the terrestrial carbon cycle: A review," *Sci. China Earth Sci.*, vol. 62, no. 10, pp. 1551–1563, Oct. 2019.
[51] Q. Wang, J. Zeng, S. Leng, B. Fan, J. Tang, C. Jiang, Y. Huang, Q. Zhang, Y. Qu, W. Wang, and W. Shui, "The effects of air temperature and precipitation on the net primary productivity in China during the early 21st century," *Front. Earth Sci.*, vol. 12, no. 4, pp. 818–833, Dec. 2018.
[52] Z. Wen-Quan, P. Yao-Zhong, and Z. Jin-Shui, "Estimation of net primary productivity of Chinese terrestrial vegetation based on remote sensing," *Chin. J. Plant Ecol.*, vol. 31, no. 3, pp. 413–424, 2007.
[53] E. Shang, E. Xu, H. Zhang, and F. Liu, "Analysis of spatiotemporal dynamics of the chinese vegetation net primary productivity from the 1960s to the 2000s," *Remote Sens.*, vol. 10, no. 6, p. 860, Jun. 2018.
[54] S. Piao, A. Mohammat, J. Fang, Q. Cai, and J. Feng, "NDVI-based increase in growth of temperate grasslands and its responses to climate changes in China," *Global Environ. Change*, vol. 16, no. 4, pp. 340–348, Oct. 2006.
[55] S. Piao, J. Fang, and J. He, "Variations in vegetation net primary production in the Qinghai–Xizang Plateau, China, from 1982 to 1999," *Climatic Change*, vol. 74, nos. 1–3, pp. 253–267, Jan. 2006.
[56] X. Feng, G. Liu, J. Chen, M. Chen, J. Liu, W. Ju, R. Sun, and W. Zhou, "Net primary productivity of China's terrestrial ecosystems from a process model driven by remote sensing," *J. Environ. Manage.*, vol. 85, no. 3, pp. 563–573, Nov. 2007.
[57] F. Pei, X. Li, X. Liu, and C. Lao, "Assessing the impacts of droughts on net primary productivity in China," *J. Environ. Manage.*, vol. 114, pp. 362–371, Jan. 2013.
[58] K. Zheng, J.-Z. Wei, J.-Y. Pei, H. Cheng, X.-L. Zhang, F.-Q. Huang, F.-M. Li, and J.-S. Ye, "Impacts of climate change and human activities on grassland vegetation variation in the Chinese Loess Plateau," *Sci. Total Environ.*, vol. 660, pp. 236–244, Apr. 2019.
[59] D. P. Turner, W. D. Ritts, W. B. Cohen, T. K. Maeirsperger, S. T. Gower, A. A. Kirschbaum, S. W. Running, M. Zhao, S. C. Wofsy, A. L. Dunn, B. E. Law, J. L. Campbell, W. C. Oechel, H. J. Kwon, T. P. Meyers, E. E. Small, S. A. Kurc, and J. A. Gamon, "Site-level evaluation of satellite-based global terrestrial gross primary production and net primary production monitoring," *Global Change Biol.*, vol. 11, no. 4, pp. 666–684, Apr. 2005.

DAN CAO received the B.S. and M.S. degrees from Henan Polytechnic University, in 2015 and 2018, respectively. She is currently pursuing the Ph.D. degree with the Aerospace Information Research Institute, Chinese Academy of Sciences, Beijing, China. She is mainly engaged in the expertise area of agriculture remote sensing and vegetation change research.

JIAHUA ZHANG received the Ph.D. degree in cartography and remote sensing from the Institute of Remote Sensing Applications, Chinese Academy of Sciences (CAS), in 1998. From 1999 to 2001, he held a postdoctoral position at the National Institute for Environmental Studies, Japan. Since January 2002, he has been a Professor with the Chinese Academy of Meteorological Sciences. Since 2012, he has been a Full Professor with the Aerospace Information Research Institute, CAS. He has published more than 150 peer review articles, 30 international conferences papers, and six books. His research interests include remote sensing big data application, deep learning, and image processing.

HAO YAN received the Ph.D. degree in cartography and remote sensing from the Institute of Remote Sensing Applications, Chinese Academy of Sciences (CAS), Beijing, China, in 2002. Since 2002, he has been a Full Professor with the National Meteorological Center, China Meteorological Administration, Beijing, China. He has published more than 50 peer review articles. His research interests include modeling of land surface parameters, carbon and water exchange of terrestrial ecosystem, and ecological monitoring and assessment.

LAN XUN received the B.S. degree in geographic information system from Shanxi Agricultural University, Jinzhong, China, in 2016, and the M.S. degree in cartography and geographical information system from China Agricultural University, Beijing, China, in 2018. She is currently pursuing the Ph.D. degree with the Aerospace Information Research Institute, Chinese Academy of Sciences, Beijing. Her main research interests include the application of remote sensing in crop classification.

SHANSHAN YANG received the B.S. and M.S. degrees from the School of Geography and Remote Sensing, Nanjing University of Information Science and Technology, in 2012 and 2015, respectively. She is currently pursuing the Ph.D. degree with the Aerospace Information Research Institute, Chinese Academy of Sciences. Her research interests include terrestrial ecosystem water use efficiency, carbon and water cycle, and ecosystem response to climate change.

YUN BAI received the B.S. degree from the Faculty of Geography and Resource Sciences, Sichuan Normal University, in 2012, the M.S. degree from the School of Geographical Sciences, Fujian Normal University, in 2015, and the Ph.D. from the Institute of Remote Sensing and Digital Earth, Chinese Academy of Sciences, in 2019. He is currently an Assistant Professor with the College of Computer Science and Technology, Qingdao University. His research interests include remote sensing of agriculture and terrestrial carbon-water budgets modeling.

SHA ZHANG received the B.S. and M.S. degrees from the College of Resource and Environmental Sciences, Hebei Normal University, in 2011 and 2015, respectively, and the Ph.D. degree from the Institute of Remote Sensing and Digital Earth, Chinese Academy of Sciences, in 2019. She holds a full-time postdoctoral position with Qingdao University. Her interests include crop mapping with remote sensing, crop yield estimation, and terrestrial ecosystem productivity simulation.

FENGMEI YAO received the Ph.D. degree in meteorology from the Institute of Atmospheric Physics, Chinese Academy of Sciences (CAS), Beijing, China, in 2005. Since August 2005, she has been an Assistant Professor with the Graduated University of Chinese Academy of Sciences. Since 2017, she has been a Full Professor with the College of Earth and Planetary Sciences, University of Chinese Academy of Sciences. She has been involved in climate change and effect on vegetation and agriculture, atmospheric environment, and disaster. She has published more than 100 peer-reviewed articles, 20 international conferences papers, and four books.

WENBIN ZHOU received the Ph.D. degree from the Institute of Shanghai Plant Physiology and Ecology, Chinese Academy of Sciences, in 2008. From 2009 to 2014, he held postdoctoral position at the Max Planck Institute of Molecular Plant Physiology. Since 2015, he has been a Full Professor with the Institute of Crop Sciences, Chinese Academy of Agricultural Sciences, Beijing, China. He is mainly engaged in the expertise area of agriculture remote sensing and vegetation change research. He has published more than ten peer review articles.